Volume 61
Number 31
21 April 2025
Pages 5677–5830

ChemComm

Chemical Communications

rsc.li/chemcomm

ISSN 1359-7345

ROYAL SOCIETY OF CHEMISTRY

FEATURE ARTICLE

Simon Specklin, Frédéric Taran *et al.*

Sydnonimines: synthesis, properties and applications in chemical biology

ChemComm

FEATURE ARTICLE

View Article Online
View Journal | View Issue

Cite this: *Chem. Commun.*, 2025, **61**, 5704

Sydnonimines: synthesis, properties and applications in chemical biology

Alfonso Fumanal Idocin, [a] Simon Specklin *[a] and Frédéric Taran *[b]

Received 28th January 2025,
Accepted 6th March 2025

DOI: 10.1039/d5cc00535c

rsc.li/chemcomm

Sydnonimines are intriguing compounds belonging to the mesoionic family. To date, only a limited number of research groups have studied their chemistry and use in organic synthesis, medicinal chemistry and chemical biology. This review aims at providing an overview of the synthesis and the properties of sydnonimines and the most recent developments in their use as tools for chemical biology. The recent discovery that sydnonimines can act as a dipole to undergo bioorthogonal click-and-release reactions with cycloalkynes has stimulated a renewed interest from the scientific community. Given the high potential of these mesoionics, we believe that major developments are to be expected in the field of bioorthogonal chemistry.

1 Introduction

Sydnonimines (**SI**), also called iminosydnones, are intriguing members of the mesoionic family, a term coined in 1949 by Baker and Ollis, amalgamating "mesomeric" and "ionic".[1] This group encompasses 5-membered dipolar heterocycles that cannot be adequately represented by a single charged structure. Well-known examples in literature include sydnones and münchnones while **SI** remain comparatively underexplored.[2]

[a] *Université Paris-Saclay, Inserm, CNRS, CEA, Laboratoire d'Imagerie Biomédicale Multimodale Paris-Saclay (BioMaps), Orsay 91401, France. E-mail: simon.specklin@cea.fr*
[b] *Département Médicaments et Technologies pour la Santé, CEA-DMTS-SCBM, Université Paris-Saclay, 91191 Gif-sur-Yvette, France. E-mail: frederic.taran@cea.fr*

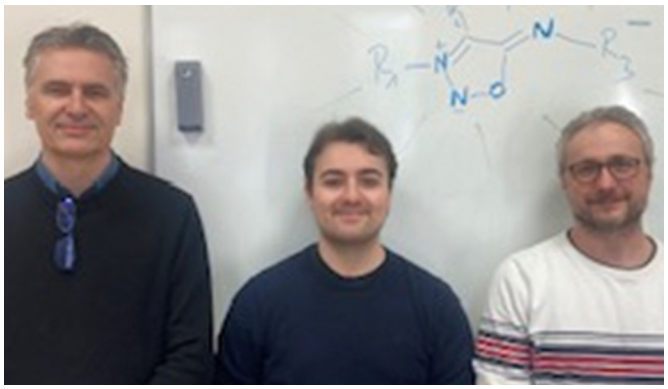

From left to right Frédéric Taran, Alfonso Fumanal Idocin, Simon Specklin

Alfonso Fumanal Idocin (middle) is a second-year PhD student at the French Alternative Energies and Atomic Energy Commission (CEA), working under the supervision of Bertrand Kuhnast, Simon Specklin, and Frédéric Taran. He secured a Marie Skłodowska-Curie fellowship as part of the ISOBIOTICS European project, which focuses on the isotopic labeling of biological drugs. His research project involves labeling these biologics with ^{18}F using a click-and-release strategy that incorporates sydnonimines.
Simon Specklin (right) is a researcher in a biomedical imaging laboratory at the French Alternative Energies and Atomic Energy Commission (CEA). After completing a PhD in chemistry at Strasbourg University under the supervision of Pr. Patrick Pale in 2010, he spent two years as a postdoctoral fellow at the organic chemistry laboratory led by Pr. Janine Cossy at ESPCI Paris. He then joined Dr Frédéric Taran group at the CEA working on bioorthogonal reactions. He later secured a permanent position at the CEA/SHFJ in 2015. His research focuses on the development of new methodologies for fluorine-18 radiolabeling of various targets, ranging from low-molecular-weight compounds to biologics.
Frédéric Taran (left) is group Leader in the department of chemistry at the French Alternative Energies and Atomic Energy Commission (CEA) located at Saclay. Dr Taran secured a PhD in chemistry at the Paris XI University under the supervision of Dr Charles Mioskowski. In 1996, he moved to a post-doctoral position with Prof. Sir Derek Barton at Texas A&M University (USA) and then came back to CEA in 1998 as permanent researcher. His research aims at developing new reagents for bioorthogonal chemistry to address important problems in the fields of bioconjugation, labelling, imaging and drug delivery.

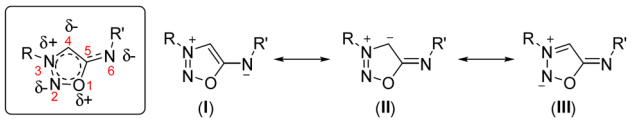

Scheme 1 Resonance structures of sydnonimines.

Structurally close to sydnones, **SI** differ by the presence of an exocyclic nitrogen instead of oxygen. Single-crystal X-ray analysis reveals that **SI** exhibit a longer exocyclic C–N bond (1.30–1.32 Å) compared to the exocyclic C–O bond in sydnones (1.19–1.22 Å), though still retaining partial C=N double-bond character, consistent with the resonance structures shown in Scheme 1.[3]

First reported in 1957,[4] **SI** initially gained attention in the 1970s for their pharmacological properties as nitric oxide (NO) donors,[5] leading to the development of several drugs, two of which remain on the market nowadays.

Beyond their biological activities, **SI** also function as ligands for metals; their deprotonation produces anionic and abnormal N-heterocyclic carbenes (NHCs),[6] allowing the formation of novel metal complexes.

There has been a resurgence of interest for **SI** in recent years related to their potential applications in chemical biology. Their role as dipoles in bioorthogonal cycloadditions has been particularly noteworthy, driving innovations in areas such as cleavable linkers for target fishing, immunoprofiling and drug delivery.

This review aims to provide a comprehensive overview of the latest advancements in **SI** research, focusing on their chemistry, biological activities, applications as metal ligands, and emerging roles in chemical biology.

2 Synthesis and functionalization of SI

2.1 General synthesis

The main synthetic route to **SI** is still the one initially published in 1957 by Brookes and Walker[4] and the team of Ohta.[7] Both teams pioneered the same synthetic pathway based on the nitrosylation of α-aminonitriles followed by cyclisation in strong acidic conditions to afford **SI**. The nitrosylation step was initially described using sodium nitrite in acidic conditions but is also alternatively carried out with alkyl nitrites. **SI** are then generated upon cyclisation with various acids, HCl being the most common, leading to **SI** as hydrochlorides. A new addition to this widely used strategy has been disclosed recently for the construction of **SI** cycles.[8] Instead of generating NO^+ *in situ* from nitrites, the work of Shuvaev *et al.* leverages the use of $NOBF_4$ salt. This reagent has a good solubility in organic media, enabling a one-step procedure for nitrosylation and subsequent cyclisation leading to **SI**. This synthetic pathway tolerates substituted α-aminonitriles and exhibits enhanced yields compared to the classical method.

All of these synthetic conditions lead to synthon **A** bearing a poorly nucleophilic amine in position 6. Functionalization of this amine, leading to **SI** mesoionic derivatives, therefore

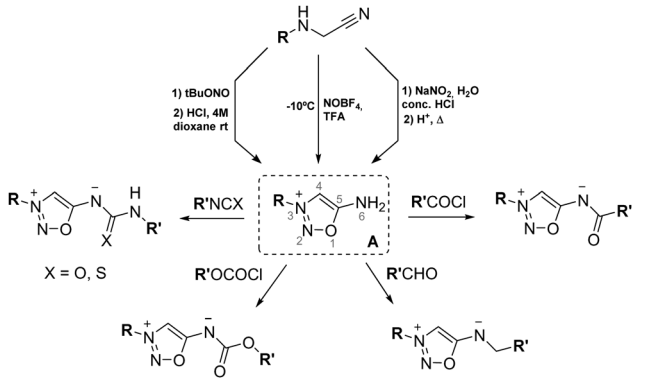

Scheme 2 General synthetic routes to sydnonimines.

requires strong electrophiles such as acylchlorides, isocyanates, chloroformates or aldehydes (Scheme 2). These functionalizations are described in detail in the following paragraph.

Recently, the team of Lamaty reported the synthesis of **SI** using mechanochemistry.[9] Starting from a primary amine, an efficient one-pot procedure leading to **SI** cyclisation was developed by vibratory milling ball grinding. The synthesis of linsidomine and feprosidnine (two bioactive **SI**, see Section 3) analogues was notably achieved in solvent free conditions with very high yields after a straightforward extraction. This method lead to **SI** as hexafluorophosphates salts, which can be interesting for applications requiring non-nucleophilic anion.

Due to the growing interest in the biological properties of **SI**, numerous derivatives have been synthesized since their discovery, expanding the chemical space of these compounds. One of the structural key points of **SI** is the exocyclic nitrogen, whose functionalization plays a crucial role in stabilizing their structure toward high pH levels. Many carbonyl derivatives were particularly synthesized leading to amides, carbamates, ureas, and thiourea functions in position 6.[10] The synthesis of these derivatives is mostly based on the reaction of **SI** salts with strong electrophiles. Sulfonyl derivatives were also described very early in the development of **SI**,[11] whereas 6-*N*-phosphorylated **SI** were only scarcely studied.[12]

An interesting approach from a retrosynthetic perspective was developed with the use of *p*-nitrophenyl carbonates as activated intermediates (Scheme 3). Reaction of these compounds with an alcohol or an amine provided a fast access to a variety of **SI** carbamates or ureas upon heating. Particularly useful for drug design, this strategy was first used to synthesize derivatives of the drug molsidomine.[13] The team of O'Hagan also used this activated intermediate for the synthesis of amino acid **SI** derivatives,[14] and for the attachment of **SI** to peptidic drugs.[15]

Based on these findings, our group reported the synthesis of another activated intermediate and generalized this retrosynthetic approach for the synthesis of diverse **SI**.[16] **SI** salts were readily converted to carbonylimidazole derivatives upon reaction with CDI. Further activation of imidazole by alkylation with MeI provided highly reactive carbonyl- and thiocarbonylimidazolium intermediates which reacted smoothly with amines (primary and

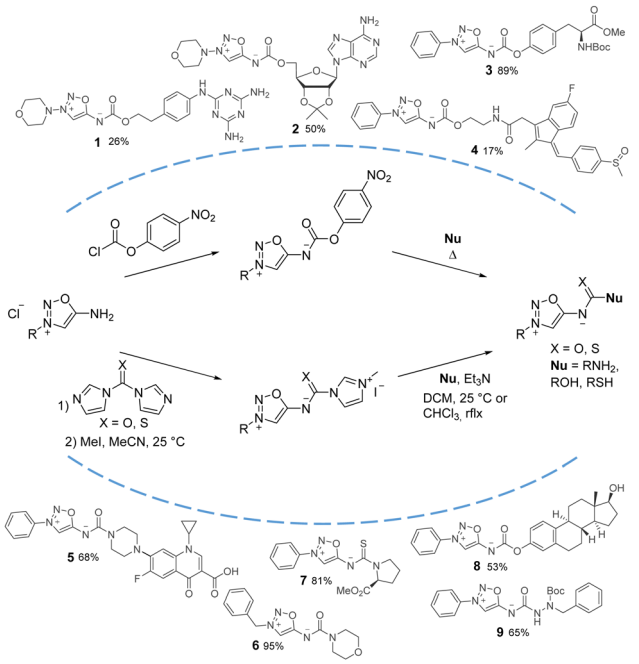

Scheme 3 Functionalization of position 6 through activated intermediates.

secondary), alcohols (aliphatic or aromatic), thiols or other nucleophiles under mild conditions. Functionalized biologically relevant compounds have also been readily substituted with a **SI** using this three steps procedure starting from **SI** hydrochlorides.[17]

6-*N*-alkyl **SI** can also be prepared using reductive amination from synthon **A**.[18] After extensive screening, sodium triacetoxyborohydride was found to be the best reducing agent for this reaction. The use of apolar and aprotic solvents was also found critical to minimize the competing ring opening of the **SI** cycle. A variety of 6-*N*-alkyl **SI** were thus reported with moderate yields from synthon **A** and aliphatic or aromatic aldehydes (Scheme 4).

Although leading to many **SI** derivatives, the synthetic pathway based on derivatization of synthon **A** cannot provide all possible structures. For instance, all arylation attempts using metal-catalyzed coupling reactions were found unsuccessful. Consequently, 3-*N*, 6-*N*-diaryl sydnonimines were never obtained until a new synthetic route was recently developed.[18] The latter was based on the cyclisation of *N*-nitrosamide intermediates obtained

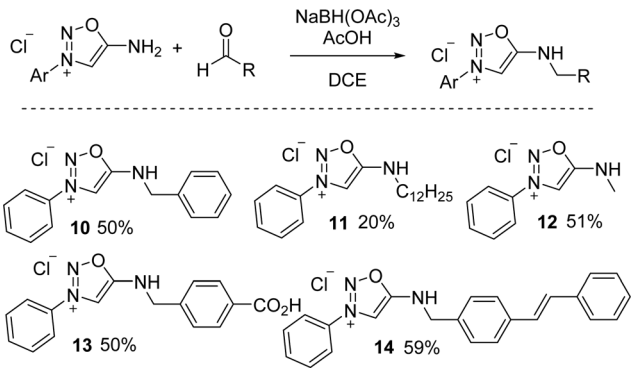

Scheme 4 Preparation of 6-*N*-alkyl **SI** by reductive amination.

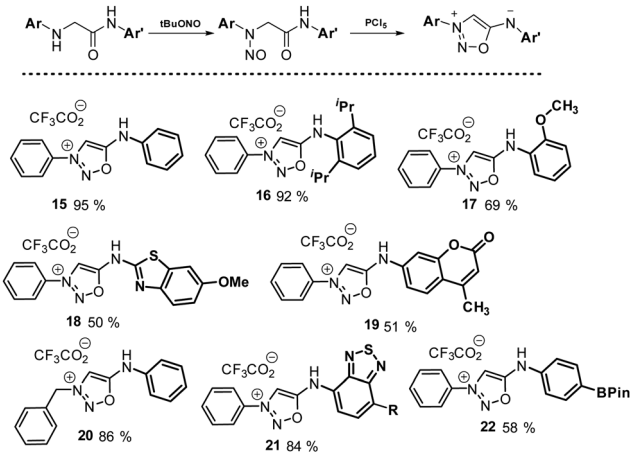

Scheme 5 Synthetic route to 3-*N*, 6-*N*-diaryl-**SI**.

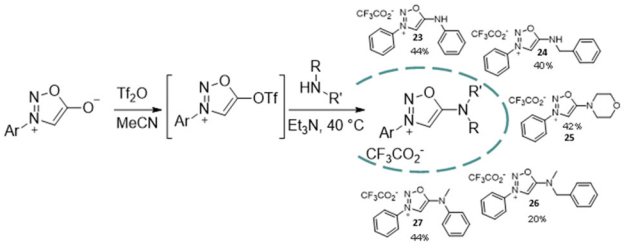

Scheme 6 Synthesis of **SI** from sydnones.

from nitrosylation of amino-amides using *tert*-butyl nitrite. After screening of several reagents, PCl_5 was identified as the most effective dehydrating reagent leading to 3,6-diaryl-**SI** in reasonable yields. This set of conditions allowed to generate a diversity of compounds with an important electronic and steric tolerance for the aryl group (Scheme 5).

However, the use of PCl_5 as a reagent limited the scope of the methodology. A complementary approach was thus developed to access diaryl-**SI** using sydnones as starting material.[19] Reaction of sydnones with Tf_2O has been described to generate the corresponding triflate in position 6 which can undergo a S_NAr reaction with carbon nucleophiles to form sydnone-methide compounds.[20] Using the same strategy with amines as nucleophiles, **SI** can be generated in mild conditions (Scheme 6). Moderate yields are obtained, due to the very high reactivity of the sydnone-triflate intermediate and the competing formation of the corresponding triflated amine. The scope of the reaction is however interesting, as primary, secondary, aliphatic and aromatic amines can be used leading to a variety of **SI** derivatives.

2.2 Functionalization in position 4-C

Functionalization in position 4 of **SI** is highly common and represents a significant part of the reports involving **SI** synthesis. This position can be substituted before the **SI** cyclisation,[21] but the most common way is to harness the specific reactivity of this position.

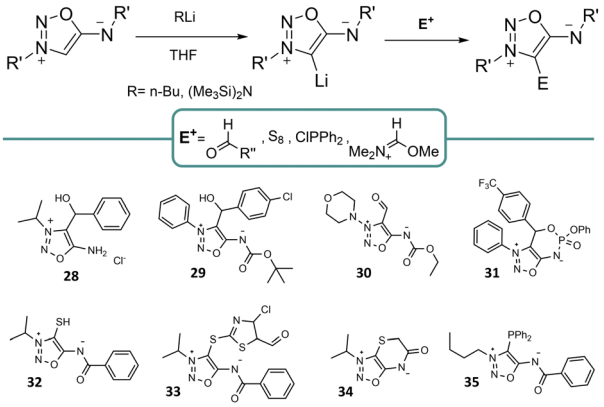

Scheme 7 Functionalization in the 4-C position of **SI**.

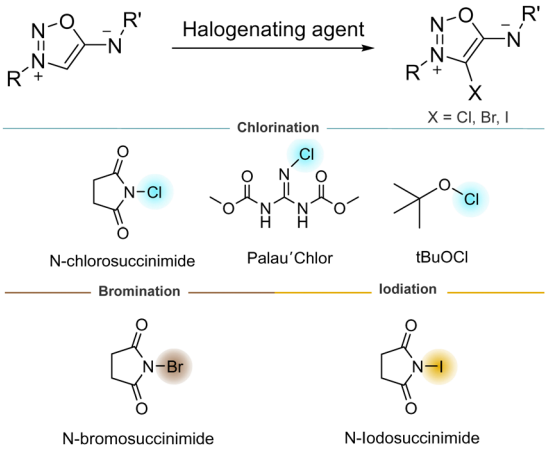

Scheme 8 Halogenation of 4-C position of **SI**.

SI can be deprotonated with a lithium base at the 4-C position resulting in a lithium adduct that can react with a variety of electrophiles (Scheme 7). Several **SI** were obtained using non-enolizable aldehydes allowing the introduction of an α-hydroxyalkyl group.[22,23] In the case of 6-*N*-phosphorus **SI** derivatives, 4-(α-hydroxy) derivatives undergo an intramolecular substitution to form a bicyclic **SI**.[12] Additionally, formylation of 4-lithiosydnnimines has been reported by DMF activation with dimethylsulfate leading to 4-formylsydnone imine. Introduction of other carbon-based substituents has been reported from 4-lithiosydnonimine,[24] which have been involved in further condensation and Knoevenagel reactions.[25]

Apart from the introduction of carbon based substituents, 4-thio derivatives of **SI** can be obtained by reaction with S_8 to generate the lithium thiolate. This species can be either alkylated to generate different 4-mercapto derivatives, which can then be oxidized to form sulfoxide derivatives,[26] or generate the 4-thiol derivative when treated with water.[27] Thiolates can also be used to form linear gold complexes or bidentate mercury complexes. However, 4-thiols seem to cleave the **SI** core where the exocyclic nitrogen atom is not substituted by electron-withdrawing groups. Lastly, 4-thio derivatives can also be intramolecularly alkylated to form bicyclic derivatives.[28] On the other hand, 4-phosphorus derivatives are synthesized by reacting the corresponding halophosphine with lithiated **SI**.[29] The corresponding **SI**-phosphine can coordinate palladium, giving rise to a five-membered metallocycle where the **SI** derivative acts as a bidentate ligand.

The position 4 of **SI** can also be easily halogenated, offering the possibility to modify their electronic properties. Overall, 4-bromo derivatives were found to be more stable and easier to synthesize than 4-chloro and 4-iodo derivatives.[30] However, our group reported a selective methodology to chlorinate the 4-C position using *t*BuOCl as chlorinating agent.[31] 4-bromo and 4-iodo derivatives, easily prepared using *N*-bromo or *N*-chlorosuccinimide, are good substrates for Suzuki and Sonogashira coupling reactions (Scheme 8).[32] To the best of our knowledge, no 4-fluoro derivative of **SI** are reported, in contrast to sydnones.[33] Halogenation of the 4-C position has proven to enhance the reactivity of **SI** as dipoles (*vide infra*), thus making this functionalization very attractive for bioorthogonal chemistry.

3 Biological activities of SI

Shortly after the initial synthesis reports of **SI**, several research groups began investigating the biological potential of this unique class of mesoionic compounds. Early screenings in the 1960s suggested a range of promising biological effects,[4] which now include antipyretic and anti-inflammatory effects,[34] monoamine oxidase (MAO) inhibition,[35] antispasmodic effects, and antitumoral activities.[36] These diverse biological applications are largely attributed to the NO-donor capabilities of **SI**, which are greatly influenced by the nature of the substituents attached to their core.

3.1 Applications as vasodilators

The vasodilatory properties of **SI** rapidly emerged as their most emblematic application. Molsidomine, a vasodilating drug developed in the 1970s, has been widely used to treat stable and unstable angina pectoris, a form of chest pain due to reduced blood flow to the heart. The active metabolite of molsidomine, **SIN-1**, was first synthesized in 1969. Researchers observed that **SIN-1** undergoes alkaline decomposition, yielding the derivative **SIN-1C**,[37] which was associated with a hypotensive effect in animals.[38] This effect was also observed in a molsidomine derivative, later identified as an effective prodrug with favorable biodistribution properties.[39] A complete mechanism for molsidomine activation was later proposed by Bohn *et al.*[40] In this mechanism, molsidomine is hydrolyzed by liver esterases to produce **SIN-1**, which is unstable at physiological pH and is converted into an open form, **SIN-1A**. **SIN-1A** then reacts with dissolved oxygen to generate nitric oxide (NO) and superoxide anion. Due to their stoichiometric release, these species can form peroxynitrite ($ONOO^-$), reducing the availability of free NO (Scheme 9).

To enhance the NO availability and reduce undesired toxic peroxynitrite formation, a hybrid molecule incorporating a radical scavenger functionality was described by Acharya *et al.*[41]

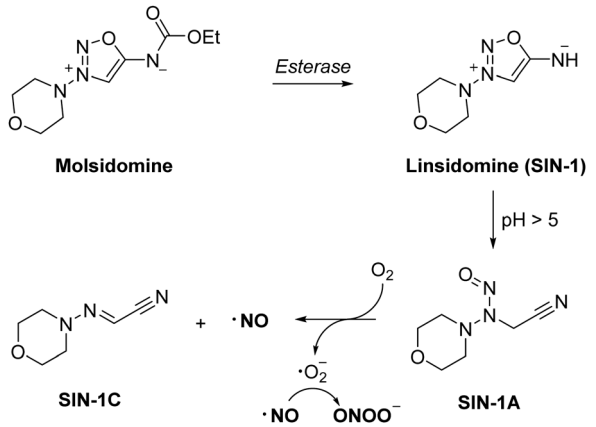

Scheme 9 Proposed mechanism for molsidomine activation *in vivo*.

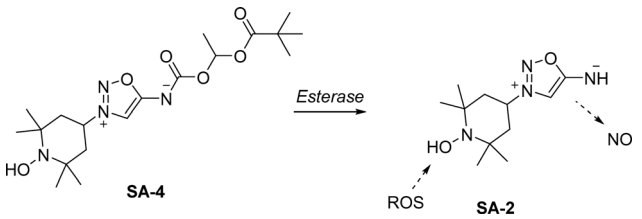

Scheme 10 Structure of a hybrid molecule containing **SI**.

The prodrug **SA-4** was developed to release **SA-2**, which demonstrated notable biological activities, including elevating superoxide dismutase levels and protecting photoreceptor cells from oxidative stress induced by H_2O_2 (Scheme 10). The same authors then demonstrated the beneficial effect of **SA-2** in preventing retinal ganglion cells death in animal models.[42]

Recently, molsidomine and acetylsalicylic acid have been combined into a hybrid molecule by Szöke *et al.* in order to increase the effect of aspirin in ischemic heart conditions and decrease gastrointestinal damage.[43] Recent studies report the synthesis of *N*-nitroso-3-morpholinosydnonimine, which can liberate two molecules of NO while reducing the generation of toxic peroxynitrite.[44] Other vasodilating drug candidates include pirsidomine and its active hydrolyzed form (darsidomine),[45,46] although they have been discarded in phase 2 trials.

3.2 Applications as plant growth stimulants

Cherepanov *et al.* reported the properties of **SI** as plant growth regulators, focusing on 4-C derivatives (Scheme 11).[23,47,48] The effect can range from herbicidal to growth stimulant depending on the dose. However, plant species and the **SI** structure (in particular the 6-*N* and 3-*N* substituents) play an important role on modulating this effect.[49] In addition, ferrocenyl-containing sydnonimines have proven to act as antidotes to herbicides such as Zinger WP.[50,51]

3.3 Applications as psychostimulants

SI containing an amphetamine moiety have psychostimulant properties with reduced toxicity and addictiveness compared to the free amphetamine.[52,53] The first psychoactive **SI** drug was mesocarb (also known as sydnocarb or MLR-1017). First developed in 1971 and commercialized until 2008, mesocarb was prescribed in Russia for psychiatric disorders.[54] Mesocarb constitutes a racemic mixture, the active enantiomer was later renamed armesocarb (MLR-1019). Armesocarb functions as a dopamine reuptake inhibitor by obstructing the dopamine transporter.[55] Feprosidnine is another psychoactive **SI** drug prescribed in Russia to treat depression. Feprosidnine differentiates from armesocarb by having the 6-N atom unsubstituted (Scheme 12).

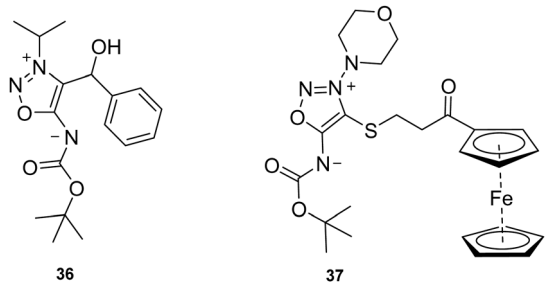

Scheme 11 Structure of **SI** with plant growth stimulation activities.

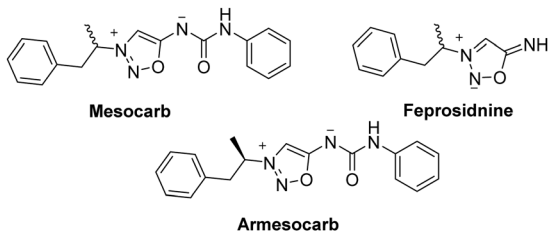

Scheme 12 Structure of **SI** with psychostimulant activities.

3.4 Applications for cancer treatment

Nitrosulindac is a well-known nitric oxide-donating non-steroidal anti-inflammatory drug (NO-NSAID), inhibiting proliferation and inducing apoptosis in human prostatic epithelial cells.[56] In 2013, O'Hagan *et al.* synthesized several **SI** analogues of nitrosulindac displaying similar or better activities than the parent drug (Scheme 13).[57]

In 2014, O'Hagan *et al.* used the NO donor properties of **SI** to enhance the biological activity of abiraterone,[15] a drug used for

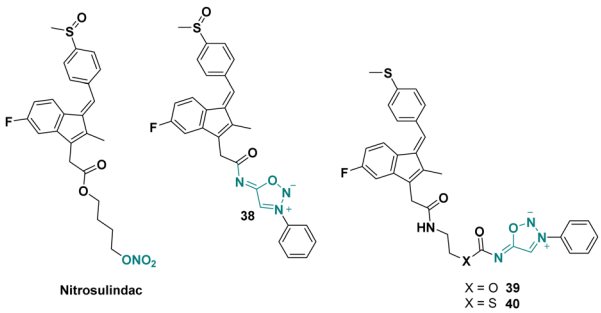

Scheme 13 Structures of **SI** analogues of nitrosulindac.

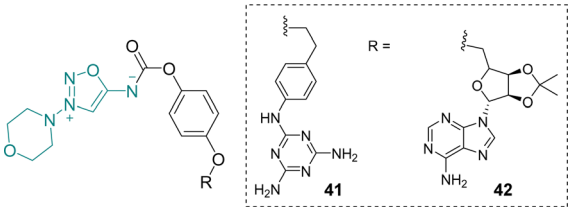

Scheme 14 Structures of **SI** with trypanocidal activities.

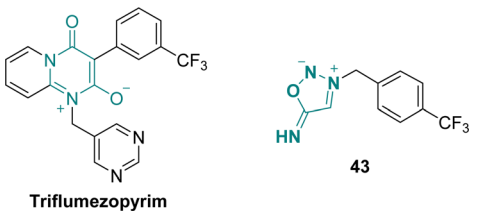

Scheme 15 Structures of **SI** analogues of triflumezopyrim.

the treatment of late stage, metastatic prostate cancer. The authors developed a molecule bearing abiraterone, **SI** and an integrin binding RGD peptide sequence presenting significant cytotoxicity towards cancer cell lines.

3.5 Applications as trypanocidal agent

In 2003, Hoffmann *et al.* reported the synthesis of several **SI** derivatives with notable trypanocidal properties.[58] The compounds were designed around an **SI** motif derived from molsidomine and incorporated purine or melaminophenyl groups, which facilitate recognition by a trypanosomal purine transporter. Their trypanocidal effects are hypothesized to result from the release of nitric oxide and superoxide, which may disrupt the parasite's cellular replication (Scheme 14).

3.6 Applications as insecticidal agent

Triflumezopyrim is a mesoionic insecticide recently developed by DuPont acting as an efficient inhibitor for the nicotinic acetylcholine receptor (Scheme 15).[59] To evaluate the role of the mesoionic structure on the biological activity, Qian *et al.* reported in 2021 several **SI** derivatives whose lethality against *Mythimna separate* are comparable to the one of the parent drug.[60]

This study provided valuable information regarding the relation between the structure of the mesoionic and its insecticidal properties, providing useful background for the design of novel mesoionic insecticides.

4 SI as metal ligands

In addition to their biological activities, sydnonimine derivatives are also studied for their ability to generate anionic N-heterocylic carbenes (NHC) and abnormal NHCs (Scheme 16). It is worth mentioning that carbene formation has been only explored with sydnonimine derivatives substituted in position 6-*N*, usually 6-*N*-acyl derivatives. These compounds are conjugated heterocyclic mesomeric betaines (CMB) which can generate both

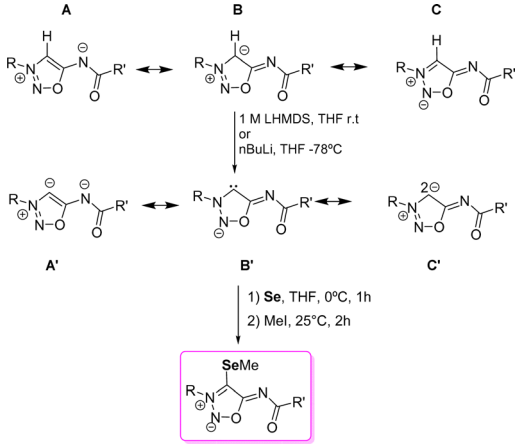

Scheme 16 Resonance forms of sydnonimines and their NHC forms. Carbene trapping with Se.

NHCs upon deprotonation of position 4-C. The resonance forms show the possibility of forming the anionic abnormal NHC (**A**′), the anionic normal NHC (**B**′), and another resonance form (**C**′) where the two negative charges are located at the 4-C carbon atom, one deallocated in the π-system and the other in the sp2 hybrid orbital.

In 2000, Cherepanov *et al.*[61] reported the first 4-lithium derivatives of **SI**, prepared by deprotonating the 4-C position with *n*BuLi; however, they noted that this approach led to the formation of unstable carbenes. Schmidt's group similarly found that deprotonation with *n*BuLi resulted in rapid degradation at room temperature. Nevertheless, treatment of **SI** with 1 M LiHMDS in THF at room temperature proved to be optimal for 4-C deprotonation, stabilizing the anionic carbene in THF for several weeks. However, more recent data suggest that this stability may be overestimated, with maximum stability at room temperature reported to last only about 10 hours.[47] Density functional theory (DFT) calculations indicated that the lithium atom positioned between the 4-C carbon and the carbonyl oxygen is essential for this stabilization, with additional influence from the substituents at the 3-N and 6-N positions. The deprotonated 4-C atom shows a ^{13}C NMR shift ranging from 142.1 ppm to 159.8 ppm, which is considered high-field for NHCs.

DFT calculations by T. Freese *et al.*[62] reveal differences in the HOMO–LUMO orbitals of the molsidomine carbene, used as an **SI** model, compared to 1,3-dimethylimidazol-2-ylidene (**44**), which represents standard NHCs. These calculations indicate altered π-accepting properties in molsidomine relative to regular NHCs, with an inversion in the HOMO orbital configuration. Specifically, the HOMO orbital in molsidomine is a π-orbital with a substantial contribution from the non-hybridized p-orbital of the 4-C atom, while the HOMO−1 corresponds to the σ-orbital typical of NHCs (see Fig. 1). Additionally, the LUMO orbitals of molsidomine are higher in energy and contain a significant coefficient from the carbene carbon atom.

The trapping of a carbene with selenium is a typical procedure to evaluate its π-acceptor strength.[63] Higher ^{77}Se NMR

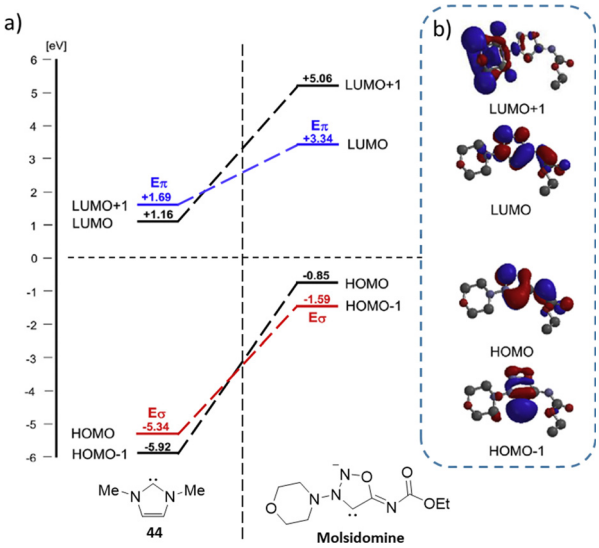

Fig. 1 (a) DFT calculation representation of frontier orbital energies of ylidene (**55** in comparison to molsidomine carbene). (b) Representation of calculated molecular orbitals of molsidomine. Reproduced from ref. 62 with permission from Elsevier, copyright 2017.

shift correlates with higher π-accepting properties of the NHC. In the case of the molsidomine selenium derivative, the NMR shift was 97.2 ppm for the 4-C carbon atom, which could be seen as a proof for the loss of π-accepting properties[63] in comparison to the model NHC. The selenium complexes have been prepared by direct reaction with selenium, followed by a methylation with MeI (Scheme 16).

Unlike sydnones, which are widely used as ligands for metals,[64,65] only few examples of NHC–metal complexes with **SI** are found in the literature (Scheme 17).

The first NHC–metal complexes obtained from **SI** carbenes were described in 2000 by Ilya A. Cherepanov and Valery N. Kalinin.[66] Direct reaction of the **SI** carbenes with CuBr afforded the corresponding Cu-complexes which were found to be good substrates for palladium-catalyzed cross-coupling reactions as seen in Scheme 18.

Gold complexes can also be prepared by direct reaction of the deprotonated **SI** with $(PPh_3)AuCl$. Only one of the two gold complexes described in the literature has crystallographic data available (Fig. 2).[62]

Mercury complexes were synthesized by trapping the carbene with $HgCl_2$ at 0 °C. The crystal structure (Fig. 3) showed the

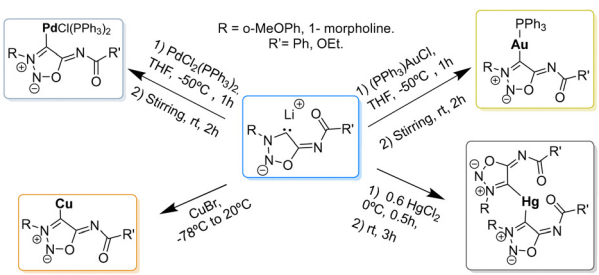

Scheme 17 Reactions of **SI** carbenes with metals.

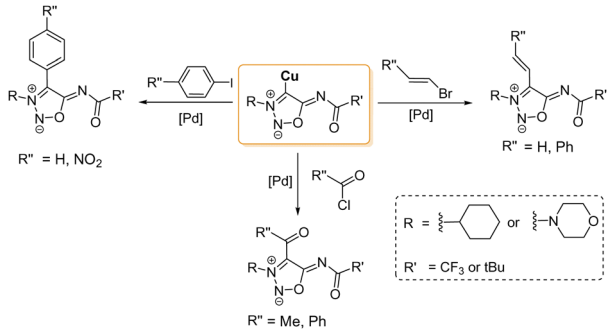

Scheme 18 Different cross-coupling reactions with 4-copper **SI** derivatives. Conditions: $Pd(PPh_3)_4$ 20 °C, 2–24 h. Yields: 30–65%.

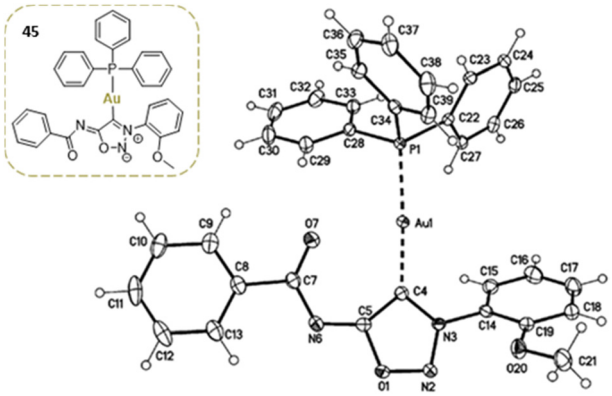

Fig. 2 Crystal structure of a sydnonimine NHC–Au complex. Reproduced from ref. 62 with permission from Elsevier, copyright 2017.

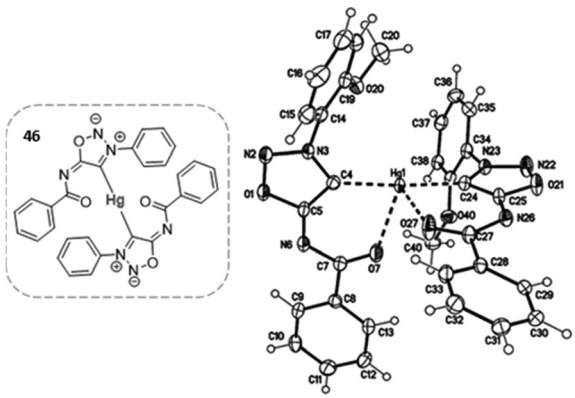

Fig. 3 Crystal structure of a sydnonimine bis(NHC)–Hg complex. Reproduced from ref. 26 with permission from Royal Society of Chemistry, copyright 2019.

coordination of the mercury atom by two **SI** carbenes, giving rise to bis-NHC complexes.[26]

On the other hand, palladium complexes have been explored to a greater extent.[26,67] Freese *et al.* reported the preparation of palladium complexes under conditions similar to those used for synthesizing gold complexes, involving the direct reaction of **SI** carbenes at low temperature. These **SI**-Pd complexes (see Scheme 19) demonstrated notable stability and proved to

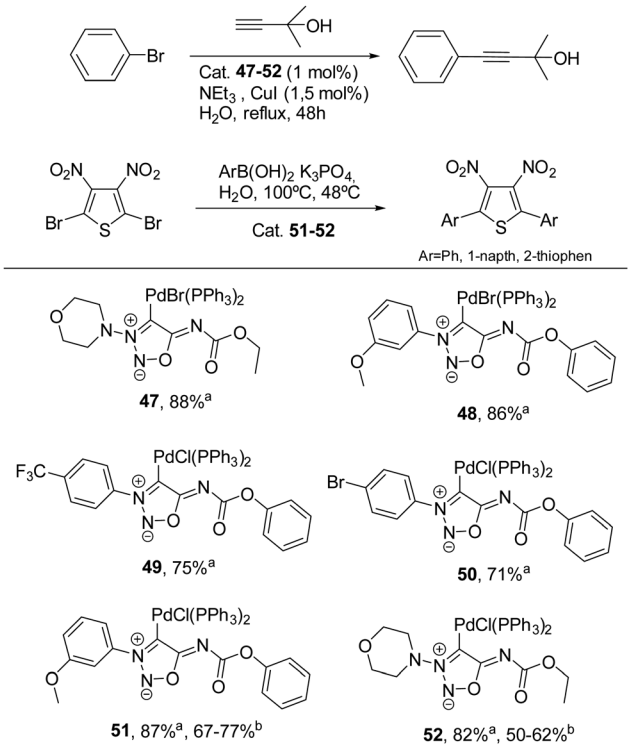

Scheme 19 Palladium sydnonimine complexes tested in Sonogashira–Hagihara and Suzuki–Miyaura reactions. [a]Yields for Sonogashira–Hagihara coupling. [b]Yields for Suzuki–Miyaura coupling.

be effective catalysts for Sonogashira–Hagihara reactions, with some complexes (**51** and **52**) also showing catalytic activity in Suzuki–Miyaura reactions.

Overall, NHC metal complexes using **SI** are scarcely reported in the literature and their applications have largely been confined to catalysis. To the best of our knowledge, no biological studies have been carried out or even proposed for these interesting complexes. This gap suggests the potential for discovering interesting applications of a group of NHC metal complexes that have not yet been explored.

5 Sydnonimines as dipoles for cycloaddition reactions

Like sydnones, sydnonimines are masked azomethine imine dipoles able to react in 1,3-dipolar cycloaddition reactions (Scheme 20).[68] This property was first reported by B. G. Yashunskii in the 60s using acrylonitrile as dipolarophile and a few years later by K. T. Potts and coworkers who described the formation of a pyrazole product upon reaction with dimethyl acetylenedicarboxylate under refluxing xylene.[69,70]

Scheme 20 Sydnones and sydnonimines are masked azomethine dipoles.

Surprisingly, following these pioneer two articles, no other paper exploited this reaction until our work published in 2017.[71] Among 25 mesoionic compounds screened for their reactivity with cyclooctynes, our group identified sydnonimines (**SI**) as suitable substrates for strained-promoted cycloaddition reactions. Notably, the reaction occurs at room temperature, yielding a pyrazole product quantitatively through the click reaction between the cyclooctyne and the azomethine imine dipole, accompanied by the release of an isocyanate (Fig. 4). The mechanism involves a (3+2) cycloaddition step, forming a bicyclic intermediate that undergoes a spontaneous retro-Diels–Alder reaction. This reaction, termed strain-promoted sydnonImine cycloaddition (SPSIC), maintains its efficiency in biological fluids such as cell lysate and blood plasma. Consequently, it emerges as a new bioorthogonal click-and-release reaction with potential applications in chemical biology.[72] Research efforts aimed at improving the reaction kinetics of SPSIC have underscored the significant influence of substrate structure on the reaction rate constants. Notably, the reaction rate can be enhanced by two orders of magnitude by increasing the strain of the cyclooctyne (Fig. 4). As expected, TMTH (tetramethylthiocycloheptyne) exhibited high reactivity towards **SI**, although its instability might be an issue. DBCO (dibenzocyclooctyne), offering a balanced compromise between reactivity and stability, is often the preferred cyclooctyne in SPSIC reactions. In addition to cyclooctynes, the structure of **SI** also significantly influences the SPSIC kinetics. Three positions on the **SI** scaffold can be modified: positions 3-N, 4-C, and 6-N. Alterations at all three positions have a tremendous impact on the reaction speed, highlighting the importance of optimizing **SI** structures to enhance the efficiency of the SPSIC reaction (Fig. 4).

Electronic effects in position 3-N and 6-N have a particularly strong impact on the reactivity of **SI**. Electron-withdrawing groups in position 3-N and electron-donating groups in position 6-N favor the active azomethine imine mesomeric form of **SI** and therefore have a beneficial impact on reaction kinetics.[73] Like sydnones,[74] the presence of a halogen atom in position 4-C also improves significantly the speed of the SPSIC reaction.[75] Among the numerous **SI** studied, 3-*N*, 6-*N*-diaryl sydnonimines appeared the most reactive under physiological conditions affording rate constants from 18 to 458 M^{-1} s^{-1} depending on aromatic substitutions.[75] 6-*N*-Alkyl sydnonimines react with lower kinetics due to higher pK_a of the amine in position 6. For instance only 4% of the reactive mesosionic form of 3-*N*-phenyl, 6-*N*-benzyl sydnonimine are present at physiological pH which explains why the rate constant is only of 59 M^{-1} s^{-1}. On the contrary 85% of this compound is deprotonated at pH 9.5 inducing an enhancement of the SPSIC rate constant up to 1220 M^{-1} s^{-1} (Fig. 5).

In addition to strained-promoted cycloadditions, 3-*N*,6-*N*-diaryl sydnonimines can also react with terminal alkynes under copper-catalysis.[76] In this case also the efficiency on this reaction is highly dependent of the **SI** structure. Although all **SI**

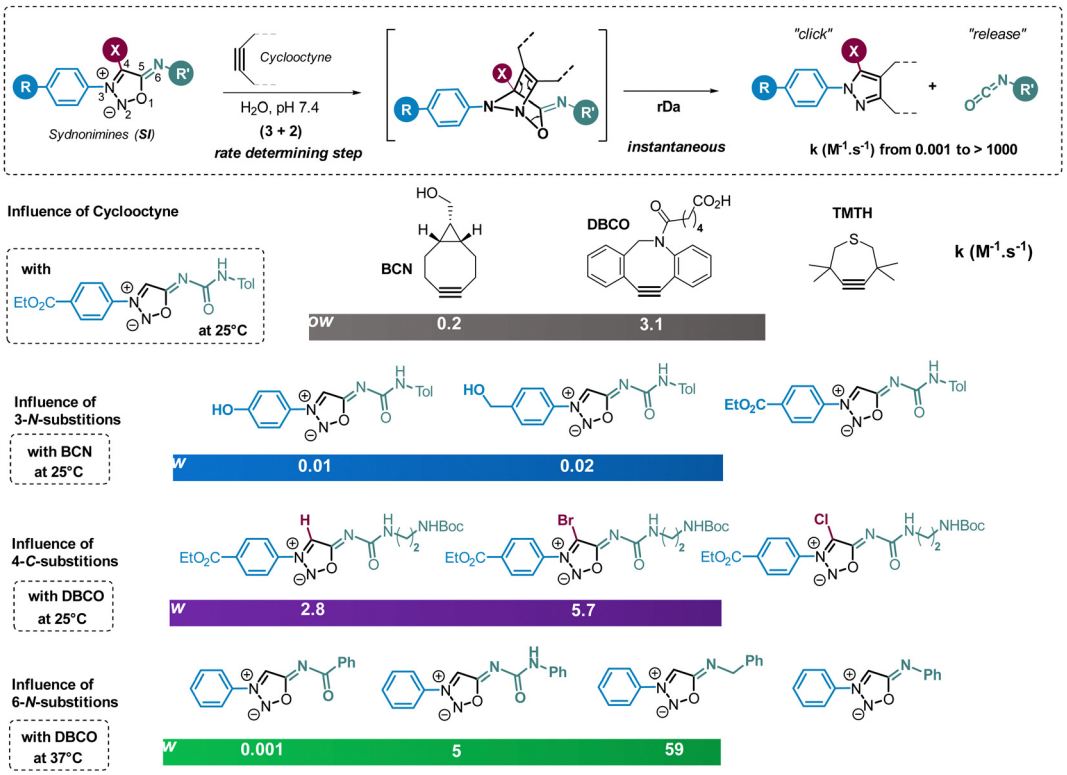

Fig. 4 Strained-promoted sydnonimine cycloaddition (SPSIC). Selected examples illustrating the influence of cyclooctyne and **SI** structures on the SPSIC kinetics.

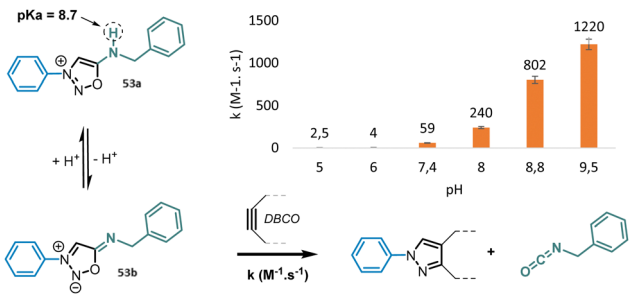

Fig. 5 Influence of pH on SPSIC reaction with 6-*N*-alkyl sydnonimines.

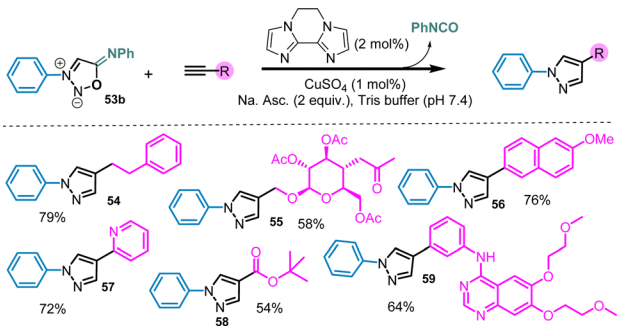

Scheme 21 Cu-catalyzed sydnonimine–alkyne cycloaddition.

bearing electron-withdrawing groups in position 6 are almost inactive, 6-*N*-aryl **SI** display very interesting reactivity toward Cu-catalyzed cycloaddition with alkynes. Only 1% of copper salts are required to catalyze efficiently the reaction which makes sydnonimines even more reactive than sydnones (Scheme 21). The reaction is preferably conducted in tris-buffer in order to quench the released isocyanate. Under these conditions, multi-functionalized substrates can be utilized, resulting in the formation of complex pyrazoles with good yields.

To take profit of the isocyanate generated from **SI** substrates during the catalytic process, a two-steps cascade reaction has been developed. Starting from amine-containing alkynes, the formed pyrazoles can then react with the released isocyanate leading to the corresponding urea. This cascade reaction was observed with various amine-containing alkynes affording the

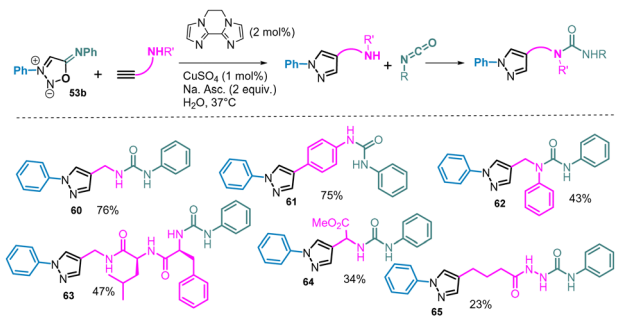

Scheme 22 Cascade reaction.

expected pyrazole-urea products in moderate to good yields (Scheme 22).

6 Application of sydnonimines in chemical biology

Because the SPSIC reaction was found to be highly efficient and relatively fast in biological fluids, its use in chemical biology has been the subject of a significant number of research. One potential drawback of the reaction relies on the release of an isocyanate which may react with biological nucleophiles, lowering the bioorthogonality of the process. To address this issue, **SI** with carbonyl or sulfonyl groups at the 6-position were initially employed for applications in chemical biology. These compounds release acyl- or sulfonyl-isocyanates, which spontaneously hydrolyze in water to form unreactive amide, urea, or sulfonamide products. An added bonus of these specific **SI** relies on their non-reactivity toward the Cu(I) catalysis.[76] This property has been used to develop bifunctional spacers able to fish and purify proteins from complex mixtures. For example sydnonimine **66** was successfully used to carry out an activity-based purification method of β-lactam targets.[77] First, a model L,D-transpeptidase was incubated with an alkynylated carbapenem substrate resulting in the formation of an acylenzyme. The alkyne group of the enzyme-bound carbapenem was then exploited for CuAAC attachment with probe **66**. After binding to streptavidin magnetic beads and purification, the SPSIC reaction with a DBCO-TAMRA derivative enabled the release and fluorescent labeling of the captured carbapenem target from the streptavidin support (Fig. 6).

The use of **SI** as bioorthogonal cleavable linker has been further explored in the field of bioconjugation. An automated technology has been notably developed to access to antibody conjugates with the precise attachment of one single payload per antibody (degree of conjugation DoC = 1).[78] In this process, excess of the native antibody is iteratively engaged into cycles of low-conversion chemical modification with the sydnonimine derivative **67**, allowing the monobiotinylation of the antibody, and subsequently immobilized onto a streptavidin column (Fig. 7). Once captured on the solid support, the antibody is detached after addition of a cyclooctyne functionalized by the drug of interest. The desired monoconjugated antibody (*i.e.*, DoC = 1) is then simply collected at the column outlet. First designed to enable mg scale syntheses of stoichiometric antibody–payload conjugates, the experimental setup has been recently adjusted to allow the manipulation of μg quantities of precious antibodies.[79]

Like sydnones,[80] **SI** can efficiently quench several fluorophores, making them valuable tools for developing fluorogenic probes. In 2020, we leveraged this property to design probes capable of generating two distinct fluorescent signals in biological media following the SPSIC reaction (Fig. 8).[81] Among the different probes, compound **68** was found the most promising. Upon reaction with DBCO, it simultaneously released two fluorescent species: naphthalimide-urea and pyrazolo-pyridinium. The reaction exhibited sufficiently fast rate constants, allowing successful application in living cells. The probe was designed to be doubly fluorogenic: upon click reaction, the resulting pyrazole exhibits greater fluorescence than **68** due to intramolecular charge transfer (ICT). Additionally, the quenching of the naphthalimide *via* photo-induced electron transfer (PeT) is suppressed, leading to a significant fluorescence enhancement of the released urea. Confocal microscopy imaging confirmed the efficiency of the

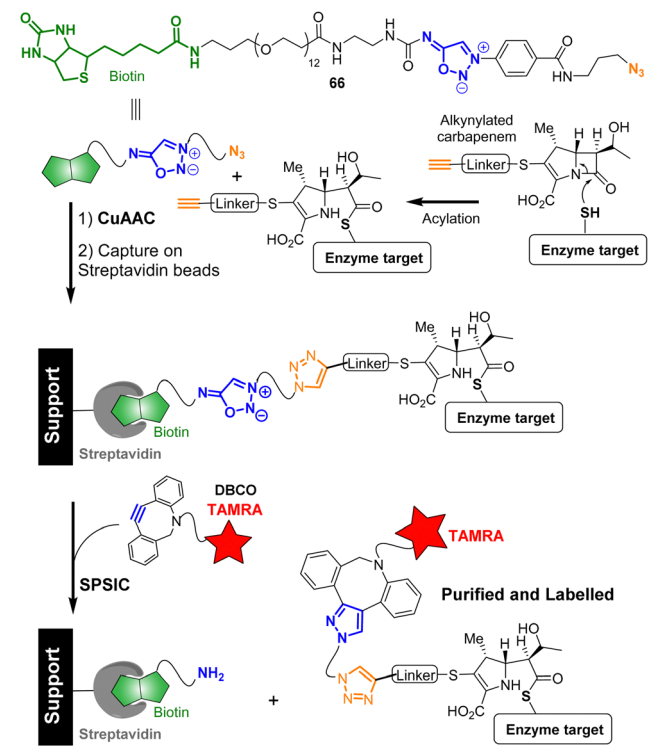

Fig. 6 **SI** as cleavable linkers for capture and release of β-lactam targets.

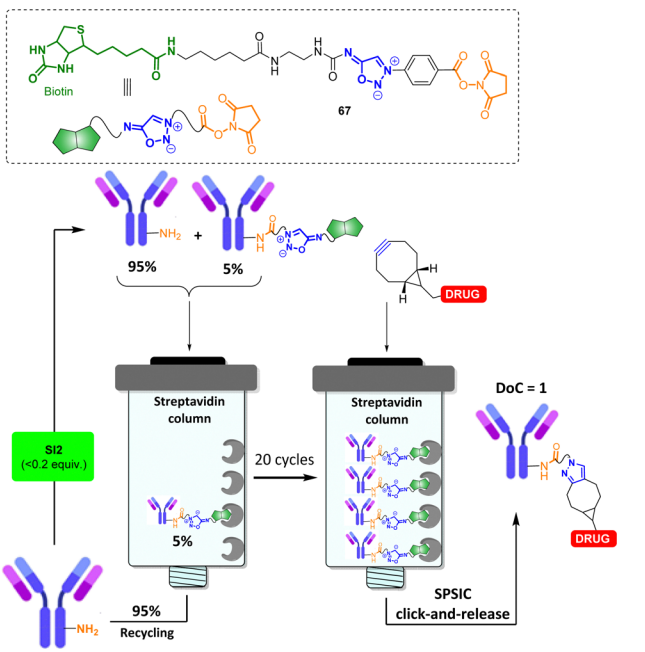

Fig. 7 Use of SPSIC to control the degree of conjugation (DoC) of antibody conjugates.

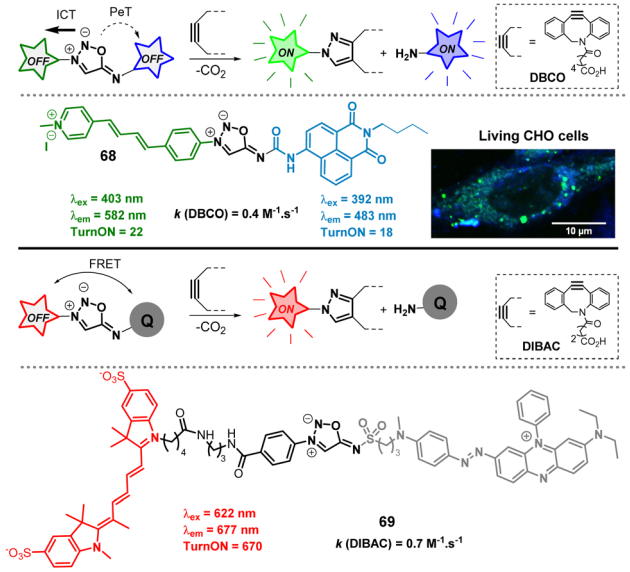

Fig. 8 Fluorogenic sydnonimines. ITC = intramolecular charge transfer, PeT = photoinduced electron tranfer; FRET = fluorescence resonance energy transfer. Adapted from ref. 81 with permission from Royal Society of Chemistry, copyright 2020.

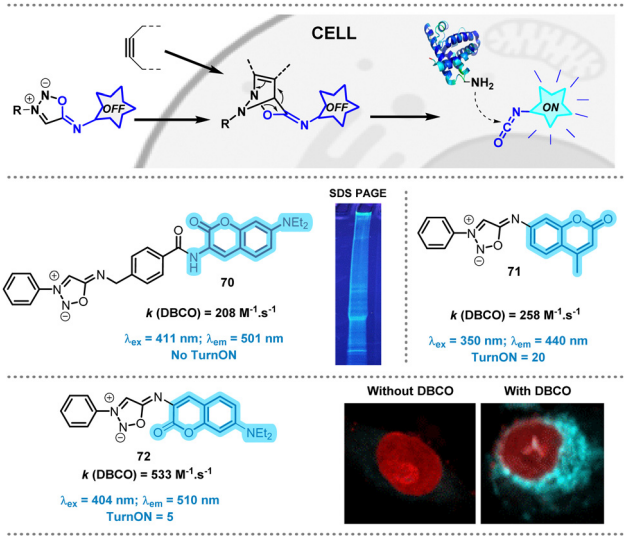

Fig. 9 Bioorthogonal release of fluorescent isocyanates in cell. Adapted from ref. 84 with permission from Royal Society of Chemistry, copyright 2024.

dual turn-on SPSIC reaction within cells, further validating the biocompatibility of the approach. Two years later, the group of Liang pursued an alternative strategy to develop even more powerful turn-on probes.[82] The design utilized quenchers attached to the 6-N position of the **SI** core to quench a fluorophore linked at the 3-N position. Among the probes, **69** bearing a Cy5 flurophore and a BHQ quencher was found to display impressive optical properties.

In 2023, our group described a new class of **SI** able to release alkyl or aryl-isocyanates in biological media.[75] This type of isocyanates are stable enough to react with bionucleophiles, including proteins. To exploit this property, several probes were developed in order to release fluorescent isocyanates inside cells (Fig. 9). Acting as caged isocyanates, these probes have the potential to label permanently biological materials within the cells which is interesting for cell imaging.[83] This has been confirmed when probe **70** was incubated with two cell models HEK293 (human embryonic kidney cells) and A549 (lung cancer cells) and further treated with DBCO. After cell lysis, SDS-PAGE analysis was performed highlighting multiple fluorescent bands on the electrophoresis gel indicating that numerous proteins inside the cells have been efficiently labeled.

Although probe **70** displayed high reactivity toward DBCO, it is not fluorogenic, making the monitoring of the SPSIC reaction in living cells difficult. In order to palliate this drawback, probes **71–72** bearing the coumarine moiety directly branched at position N-6 of the **SI** core were designed. Both displayed impressive kinetics and exploitable turn-on when mixed with DBCO. **72** was found the most suitable for cell imaging: its high reactivity allowed complete release of coumarin-isocyanate in 30 min inside A549 cells (Fig. 9).[84] The fluorescent labelling was resistant to several successive washing steps suggesting irreversible labelling of the cells.

Prodrug strategies utilizing bioorthogonal bond cleavage chemistry have emerged as a promising therapeutic approach, offering significant advantages over traditional prodrug methods, such as a precise spatiotemporal control of drug activation.[85] In this context, **SI** have been used to mask amide, sulfonamide and urea-containing drugs. Liang *et al.* pioneered this approach by developing a **SI** capable of releasing the sulfonamide drug Celecoxib through bioorthogonal reaction with DBCO (Fig. 10).[86] Following this work, the same group used a similar **SI**-based prodrug to deliver Celecoxib into the mitochondria of HeLa and HepG2 cancer cells. The study indicated that celecoxib-induced cancer cell death may not involve mitochondria-related pathway.[87] One limitation of

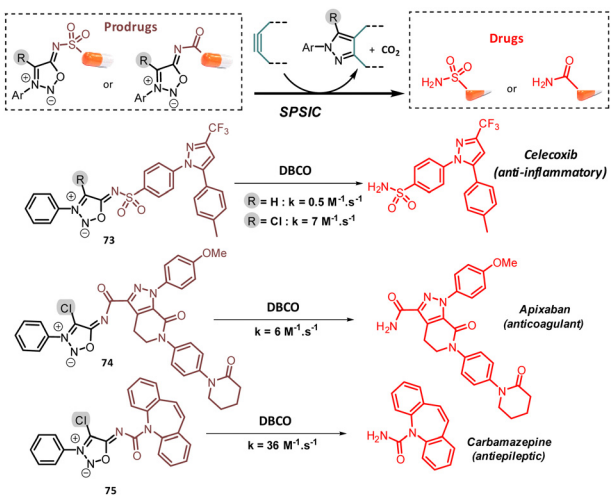

Fig. 10 Drug release from **SI**-prodrugs.

these **SI** is their slow kinetics in drug release. To address this, our group developed a method to chlorinate the 4-C position of **SI** enhancing their reactivity as dipole.[88] The resulting chlorosydnonimines demonstrated much higher reactivity, enabling faster release of drugs containing a terminal sulfonamide, urea and even amide functions. The latter reacted smoothly, with rate constants $k > 1\ M^{-1}\ s^{-1}$, whereas their non-chlorinated counterparts were nearly unreactive, highlighting the dramatic beneficial influence of the chlorine atom on **SI** reactivity.

Although several bioorthogonal reactions are efficient and useful when performed *in vitro* in biological media and even inside cells, only a few were successfully applied *in vivo*. In addition to bioorthogonality, biostability, non-toxicity, favorable pharmacokinetics and high reaction kinetics are essential prerequisites for *in vivo* applications. The SPSIC is one of the few reactions that has demonstrated effectiveness in animal models. In 2019, our group provided the first proof-of-concept for the utility of the SPSIC reaction *in vivo*. We developed a dual tumor-targeting strategy using micelles constructed from the amphiphile **76** containing a **SI** moiety, which separates the PEG head from the lipophilic chain (Fig. 11).[89]

Addition of lipophilic cyclooctynes to these micelles induces a high local concentration of both cyclooctyne and **76** inside the micelle core leading to fast cleavage of the amphiphile and micelle disassembly in only a few seconds. To ensure that micelle decomposition and subsequent content release (*e.g.*, fluorophore or drug) occur specifically at the tumor site, we employed a hydrophilic β-glucuronidase-responsive proactivator (**DBCO-Glu**). Because of its hydrophilicity, this cyclooctyne is inactive toward the micelle. The activation of **DBCO-Glu** at the tumor is triggered by β-glucuronidase, an enzyme overexpressed by cancer cells, inducing the detachment of the hydrophilic part of **DBCO-Glu** to form active **DBCO-NH$_2$**. Once activated, the bioorthogonal reaction proceeds, resulting in micelle destruction. This strategy was first demonstrated in mice using micelles loaded with a dye. 24 h after micelle injection, tumor accumulation was observed, and the proactivator **DBCO-Glu** was subsequently injected, causing the micelles to disassemble and release the dye into malignant tissues. Few years later, this strategy was successfully applied to the release of the anticancer drug Entinostat within cancer cells. An interesting enhancement of the biological activity of

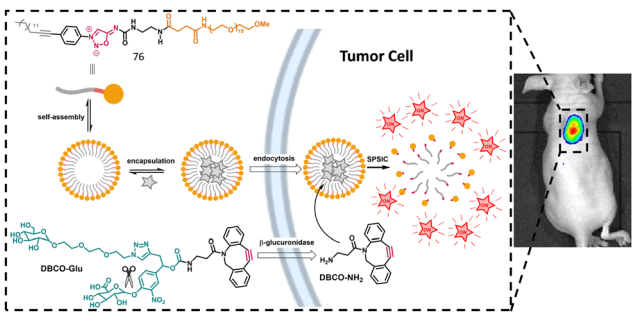

Fig. 11 Drug release from cleavable micelles. Adapted from ref. 89 with permission from Wiley, copyright 2019.

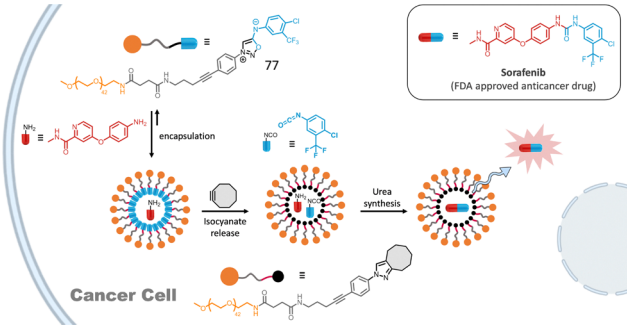

Fig. 12 SPSIC-promoted drug construction inside cancer cells. Adapted from ref. 91 with permission from Wiley, copyright 2025.

the drug was observed using this strategy.[90] Very recently, micelles constructed with amphiphile **77** allowed the synthesis of a bioactive urea in cancer cells (Fig. 12).[91] Upon SPSIC reaction, **77** releases an isocyanate which reacts rapidly with an encapsulated amine yielding the corresponding urea in the hydrophobic core of the micelles. Application of this strategy was made with the synthesis of the FDA-approved anticancer drug Sorafenib inside living cells. Interestingly, this work proved that bioorthogonal chemistry coupled with confinement could make non-bioorthogonal transformations possible inside living cells.

Recently, Liu and Zhang demonstrated the use of SPSIC for *in vivo* cancer photothermal therapy (PTT).[92] The authors described a strategy based on the injection of two gold nanoparticles: **AuNP-1** functionalized by PEGs, cyclooctynes and the tumor-targeting peptide RGD, and **AuNP-2** bearing the prodrug sydnonimine-lonidamine **78** (Fig. 13). **AuNP-1** were first intravenously injected to mice bearing the breast tumor model 4T1, leading to good tumor-specific enrichment and retention. Then, **AuNP-2** were intravenously injected. Once both AuNPs accumulated at the tumor, they react together *via* SPSIC inducing the formation of Au nanoparticles aggregates and the release of Lonidamine, a drug known to render cancer cells more sensitive to PTT. Mice were then irradiated at 808 nm for PTT treatment. The aggregated AuNPs and the release of Lonidamine showed a synergistic effect leading to significant enhancement of PTT effect and a robust tumor suppression.

Recently, our group described a multiplexed diagnostic approach based on MS-tagged antibodies cleavable by the

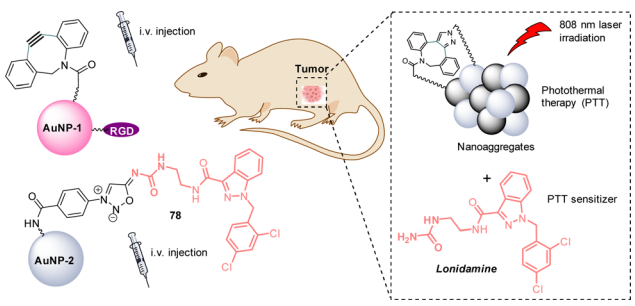

Fig. 13 Use of the SPSIC reaction for enhanced photothermal therapy.

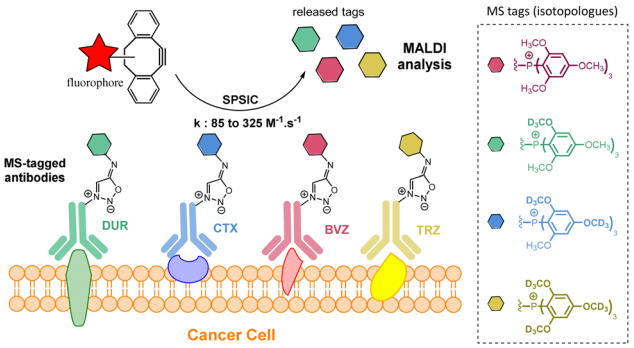

Fig. 14 Multiplexed detection of cell membrane receptors using SPSIC. Adapted from ref. 93 with permission from Royal Society of Chemistry, copyright 2024.

SPSIC reaction.[93] The technology is based on the use MS-tag isotopologues attached to anti-cancer antibodies through a **SI** linker (Fig. 14). Four FDA-approved therapeutic antibodies raised against biomarkers located at the surface of cancer cells: trastuzumab (TRZ, anti-Her2), Cetuximab (CTX, anti-EGFR), Durvalumab (DUR, anti-PDL1) and Bevacizumab (BVZ, anti-VEGF) were labelled with tris(2,4,6,-trimethoxyphenyl)-phosphonium (TMPP) tags containing a specific number of deuterium atoms. The mixture of four antibodies was then incubated on cancer cells and after washing, a DBCO-TAMRA derivative was added resulting in both fluorescent labeling of the cells and the release of the TMPP tags which can then be quantified by one single mass spectrometry analysis.

In a proof of concept studies, we then demonstrated the potential of this approach for cancer immunoprofiling in tissues and even *in vivo*. The cocktail of the four antibodies was intravenously injected to mice bearing A431 tumors. Three days later, an excess of DBCO was administered intratumorally. The released TMPP tags were subsequently quantified in the urine of the mice, showing the overexpression of the EGFR, as expected for an A431 tumor model.

Although still at an early of proof-of-concept stage, this work suggests that *in vivo* tumor characterization may be feasible, opening up promising avenues for diagnostic applications.

Conclusions

After extensive development in the 1970s as NO donors, which led to the commercialization of several drugs for various diseases, sydnonimines (**SI**) were largely overlooked for nearly 50 years. As a result, only a few synthetic methods exist, and significant synthetic efforts will be necessary to expand the diversity and complexity of **SI** structures. A key challenge in the coming years will be to develop robust and efficient synthetic routes for preparing libraries of **SI**, enabling their screening for various biological applications. The primary biological mechanism of action of many **SI** is associated with their property to release NO. Future research could explore alternative biological activities. Additionally, the polar heterocyclic nature of **SI** makes it a promising structural analogue of five-membered-ring drugs, offering valuable potential in medicinal chemistry. The recent discovery of the ability of **SI** to undergo efficient click-and-release reactions in biological media has renewed interest in these compounds. **SI** now offer promising possibilities for cleaving molecules, releasing compounds from antibodies, and breaking down nanoparticles *in vivo*, inspiring ambitious future applications in both therapeutic and diagnostic fields. With rate constants reaching up to 10^3 M^{-1} sec^{-1} and no side reactions, leading to 100% release, the SPSIC reaction can be considered as a valuable complementary tool to the widely used inverse electron-demand Diels–Alder (iEDDA) click-and-release reaction involving tetrazines and carbamate-*trans*-cyclooctenes derivatives.[94] While SPSIC has been explored in *in vivo* applications, it has not yet achieved the same level of success as iEDDA, which have led to the development of a therapeutic treatment for cancer in humans,[95] currently in phase 2. The good stability of most sydnonimines in biological media, a weak point of many tetrazines, could be a game changer. In this regard, future *in vivo* stability studies of these mesoionic compounds will be crucial to further assess their therapeutic potential.

Data availability

No primary research results, software or code have been included and no new data were generated or analyzed as part of this review.

Conflicts of interest

There are no conflicts to declare.

Acknowledgements

All authors are participant in the EU DN ISOBIOTICS Consortium. The ISOBIOTICS project has received funding from the European Union's Horizon 2020 research and innovation program under the Marie Skłodowska-Curie grant agreement no. 101072780.

Notes and references

1 W. Baker, W. D. Ollis and V. D. Poole, *J. Chem. Soc.*, 1949, 307–314.
2 K. Porte, M. Riomet, C. Figliola, D. Audisio and F. Taran, *Chem. Rev.*, 2021, **121**, 6718–6743.
3 C. R. Groom, I. J. Bruno, M. P. Lightfoot and S. C. Ward, *Acta Crystallogr.*, 2016, **B72**, 171–179.
4 P. Brookes and J. Walker, *J. Chem. Soc.*, 1957, 4409–4416.
5 Y. Asahi, K. Shinozaki and M. Nagaoka, *Chem. Pharm. Bull.*, 1971, **19**, 1079–1088.
6 T. Freese, A.-L. Lücke, J. C. Namyslo, M. Nieger and A. Schmidt, *Eur. J. Org. Chem.*, 2018, 1646–1654.
7 H. Kato, M. Hashimoto and M. Ohta, *Nippon Kagaku Zasshi*, 1957, **78**, 707.
8 A. D. Shuvaev, E. S. Zhilin and L. L. Fershtat, *Synthesis*, 2023, 1863–1874.
9 N. Pétry, F. Luttringer, X. Bantreil and F. Lamaty, *Faraday Discuss.*, 2023, **241**, 114–127.
10 V. G. Yashunskii and L. E. Kholodov, *Russ. Chem. Rev.*, 1980, **49**, 28–45.

11 H. U. Daeniker and J. Druey, *Helv. Chim. Acta*, 1962, **45**, 2462–2465.
12 A. S. Samarskaya, I. A. Cherepanov, I. A. Godovikov, A. O. Dmitrienko, S. K. Moiseev, V. N. Kalinin and E. Hey-Hawkins, *Tetrahedron*, 2018, **74**, 2693–2702.
13 L. Soulère, P. Hoffmanna and F. Bringaud, *J. Heterocycl. Chem.*, 2003, **40**, 943–947.
14 A. Nortcliffe, N. P. Botting and D. O'Hagan, *Org. Biomol. Chem.*, 2013, **11**, 4657–4671.
15 A. Nortcliffe, I. N. Fleming, N. P. Botting and D. O'Hagan, *Tetrahedron*, 2014, **70**, 8343–8347.
16 M. Riomet, K. Porte, L. Madegard, P. Thuéry, D. Audisio and F. Taran, *Org. Lett.*, 2020, **22**, 2403–2408.
17 C. Kitoun, M. Fonvielle, N. Sakkas, M. Lefresne, F. Djago, Q. Blancart Remaury, P. Poinot, M. Arthur, M. Etheve-Quelquejeu and L. Iannazzo, *Org. Lett.*, 2020, **22**, 8034–8038.
18 M. Ribéraud, K. Porte, A. Chevalier, L. Madegard, A. Rachet, A. Delaunay-Moisan, F. Vinchon, P. Thuéry, G. Chiappetta, P. A. Champagne, G. Pieters, D. Audisio and F. Taran, *J. Am. Chem. Soc.*, 2023, **145**, 2219–2229.
19 J. Baudet, E. Lesur, M. Ribéraud, A. Chevalier, T. D'Anfray, P. Thuéry, D. Audisio and F. Taran, *Chem. Commun.*, 2024, **60**, 3657–3660.
20 S. Mummel, F. Lederle, E. G. Hübner, J. C. Namyslo, M. Nieger and A. Schmidt, *Angew. Chem., Int. Ed.*, 2021, **60**, 18882–18887.
21 J. M. Ruxer, J. Mauger, D. Bénard and C. Lachoux, *J. Heterocycl. Chem.*, 1995, **32**, 643–654.
22 I. A. Cherepanov and V. N. Kalinin, *Mendeleev Commun.*, 2000, **10**, 181–182.
23 N. V. Kalganova, A. F. Smolyakov, S. K. Moiseev, M. A. Cherevatskaya and I. A. Cherepanov, *Russ. Chem. Bull.*, 2023, **72**, 1688–1700.
24 I. A. Cherepanov, L. H. Kusaeva, I. A. Godovikov and V. N. Kalinin, *Russ. Chem. Bull.*, 2009, **58**, 2474–2477.
25 I. A. Cherepanov, E. D. Savin, N. G. Frolova, M. O. Shishkova, I. A. Godovikov, K. Yu Suponitsky, K. A. Lyssenko and V. N. Kalinin, *Mendeleev Commun.*, 2009, **19**, 320–321.
26 T. Freese, J. C. Namyslo, M. Nieger and A. Schmidt, *RSC Adv.*, 2019, **9**, 4781–4788.
27 I. A. Cherepanov, S. N. Lebedev, A. S. Samarskaya, I. A. Godovikov, Y. V. Nelyubina and V. N. Kalinin, *Mendeleev Commun.*, 2009, **19**, 322–323.
28 I. A. Cherepanov, A. S. Samarskaya, R. G. Nosov, I. A. Godovikov, Y. V. Nelyubina and V. N. Kalinin, *Mendeleev Commun.*, 2014, **24**, 386–387.
29 V. N. Kalinin, S. N. Lebedev, I. A. Cherepanov, I. A. Godovikov, K. A. Lyssenko and E. Hey-Hawkins, *Polyhedron*, 2009, **28**, 2411–2417.
30 M. Goetz, K. Grozinger and J. T. Oliver, *J. Med. Chem.*, 1973, **16**, 671–673.
31 M. Feng, L. Madegard, M. Riomet, M. Louis, P. A. Champagne, G. Pieters, D. Audisio and F. Taran, *Chem. Commun.*, 2022, **58**, 8500–8503.
32 M. Riomet, E. Decuypere, K. Porte, S. Bernard, L. Plougastel, S. Kolodych, D. Audisio and F. Taran, *Chem. – Eur. J.*, 2018, **24**, 8535–8541.
33 H. Liu, D. Audisio, L. Plougastel, E. Decuypere, D.-A. Buisson, O. Koniev, S. Kolodych, A. Wagner, M. Elhabiri, A. Krzyczmonik, S. Forsback, O. Solin, V. Gouverneur and F. Taran, *Angew. Chem., Int. Ed.*, 2016, **55**, 12073–12077.
34 H. U. Daeniker and J. Druey, *Helv. Chim. Acta*, 1962, **45**, 2426–2441.
35 V. Z. Gorkin, V. G. Yashunskii, M. D. Mashkovskii, R. A. Al'tshuler, I. V. Verevkina and L. E. Kholodov, *J. Med. Chem.*, 1971, **14**, 1013–1015.
36 A. Nortcliffe, A. G. Ekstrom, J. R. Black, J. A. Ross, F. K. Habib, N. P. Botting and D. O'Hagan, *Bioorg. Med. Chem.*, 2014, **22**, 756–761.
37 Y. Asahi, K. Shinozaki and M. Nagaoka, *Chem. Pharm. Bull.*, 1971, **19**, 1079–1088.
38 K. Kikuchi, M. Hirata, A. Nagaoka and Y. Aramaki, *Jpn. J. Pharmacol.*, 1970, **20**, 23–43.
39 S. Tanayama, T. Fujita, Y. Shirakawa and Z. Suzuoki, *Jpn. J. Pharmacol.*, 1970, **20**, 413–423.
40 H. Bohn and K. Schönafinger, *J. Cardiovasc. Pharmacol.*, 1989, **14**, S6.
41 S. Acharya, P. Rogers, R. R. Krishnamoorthy, D. L. Stankowska, H. V. R. Dias and T. Yorio, *Bioorg. Med. Chem. Lett.*, 2016, **26**, 1490–1494.
42 D. L. Stankowska, A. Dibas, L. Li, W. Zhang, V. R. Krishnamoorthy, S. H. Chavala, T. P. Nguyen, T. Yorio, D. Z. Ellis and S. Acharya, *Invest Ophthalmol. Visual Sci.*, 2019, **60**, 3064–3073.
43 K. Szőke, A. Czompa, I. Lekli, P. Szabados-Fürjesi, M. Herczeg, M. Csávás, A. Borbás, P. Herczegh and Á. Tósaki, *Eur. J. Pharm. Sci.*, 2019, **131**, 159–166.
44 N. Saffon-Merceron, C. Lherbet and P. Hoffmann, *Molbank*, 2024, M1886.
45 C. L. Wainwright and P. A. Martorana, *J. Cardiovasc. Pharmacol.*, 1993, **22**(Suppl 7), S44–S50.
46 K. Ivanova, M. Schaefer, C. Drummer and R. Gerzer, *Eur. J. Pharmacol., Mol. Pharmacol. Sect.*, 1993, **244**, 37–47.
47 I. A. Cherepanov, E. V. Shevaldina, D. A. Lapshin, Y. Ya Spiridonov, V. A. Abubikerov and S. K. Moiseev, *J. Organomet. Chem.*, 2021, **943**, 121841.
48 N. V. Kalganova, N. G. Frolova, I. A. Godovikov, A. F. Smol'yakov, D. A. Lapshin and I. A. Cherepanov, *J. Organomet. Chem.*, 2024, **1005**, 122975.
49 Yu. Ya Spiridonov, I. A. Cherepanov, V. A. Abubikerov, I. Yu. Spiridonova, N. V. Kalganova, N. G. Frolova and S. K. Moiseev, *Russ. Agric. Sci.*, 2022, **48**, S63–S68.
50 E. V. Shevaldina, V. A. Tsyganov, N. V. Kalganova, A. F. Smol'yakov, N. G. Frolova and I. A. Cherepanov, *Appl. Organomet. Chem.*, 2023, **37**, e6981.
51 N. V. Kalganova, N. G. Frolova, I. A. Godovikov, A. F. Smol'yakov, E. G. Kononova and I. A. Cherepanov, *Appl. Organomet. Chem.*, 2024, **38**, e7471.
52 V. Bashkatova, A.-M. Mathieu-Kia, C. Durand and J. Penit-Soria, *Ann. N. Y. Acad. Sci.*, 2002, **965**, 180–192.
53 J. M. Witkin, N. Savtchenko, M. Mashkovsky, M. Beekman, P. Munzar, M. Gasior, S. R. Goldberg, J. T. Ungard, J. Kim, T. Shippenberg and V. Chefer, *J. Pharmacol. Exp. Ther.*, 1999, **288**, 1298–1310.
54 S. L. Erdö, B. Kiss and B. Rosdy, *Pol. J. Pharmacol. Pharm.*, 1981, **33**, 141–147.
55 S. Aggarwal, M. H. Cheng, J. M. Salvino, I. Bahar and O. V. Mortensen, *Biomedicines*, 2021, **9**, 634.
56 S. Huguenin, J. Fleury-Feith, L. Kheuang, M.-C. Jaurand, M. Bolla, J.-P. Riffaud, D. K. Chopin and F. Vacherot, *Prostate*, 2004, **61**, 132–141.
57 A. Nortcliffe, A. G. Ekstrom, J. R. Black, J. A. Ross, F. K. Habib, N. P. Botting and D. O'Hagan, *Bioorg. Med. Chem.*, 2014, **22**, 756–761.
58 L. Soulère, P. Hoffmanna and F. Bringaud, *J. Heterocycl. Chem.*, 2003, **40**, 943–947.
59 D. Cordova, E. A. Benner, M. E. Schroeder, C. W. Holyoke, W. Zhang, T. F. Pahutski, R. M. Leighty, D. R. Vincent and J. C. Hamm, *Insect Biochem. Mol. Biol.*, 2016, **74**, 32–41.
60 S. Du, X. Hu, M. Li, X. Jiang, X. Xu, J. Cheng and X. Qian, *Bioorg. Med. Chem. Lett.*, 2021, **46**, 128120.
61 I. A. Cherepanov and V. N. Kalinin, *Mendeleev Commun.*, 2000, **10**, 181–182.
62 T. Freese, A.-L. Lücke, C. A. S. Schmidt, M. Polamo, M. Nieger, J. C. Namyslo and A. Schmidt, *Tetrahedron*, 2017, **73**, 5350–5357.
63 A. Liske, K. Verlinden, H. Buhl, K. Schaper and C. Ganter, *Organometallics*, 2013, **32**, 5269–5272.
64 D. E. Vita, M. A. Schiel, M. J. Lo Fiego and G. F. Silbestri, *Organometallics*, 2024, **43**, 191–201.
65 X. Bantreil, N. Pétry and F. Lamaty, *Dalton Trans.*, 2019, **48**, 15753–15761.
66 I. A. Cherepanov and V. N. Kalinin, *Mendeleev Commun.*, 2000, **10**, 181–182.
67 A.-L. Lücke, L. Pruschinski, T. Freese and A. Schmidt, *ARKIVOC*, 2020, **2020**, 94–104.
68 R. J. Huisgen, *Org. Chem.*, 1976, **41**, 403.
69 V. F. Vasil'eva and B. G. Yashunskii, *Zh. Obshch. Khim.*, 1964, **34**, 702.
70 K. T. Potts, S. Usain and S. Husai, *J. Chem. Soc. D*, 1970, 1360–1361.
71 S. Bernard, D. Audisio, M. Riomet, S. Bregant, A. Sallustrau, L. Plougastel, E. Decuypere, S. Gabillet, R. A. Kumar, J. Elyian, M. N. Trinh, O. Koniev, A. Wagner, S. Kolodych and F. Taran, *Angew. Chem., Int. Ed.*, 2017, **56**, 15612–15616.
72 X. Ji, Z. Pan, B. Yu, L. K. De La Cruz, Y. Zheng, B. Ke and B. Wang, *Chem. Soc. Rev.*, 2019, **48**, 1077–1094.
73 M. Riomet, E. Decuypere, K. Porte, S. Bernard, L. Plougastel, S. Kolodych, D. Audisio and F. Taran, *Chem. – Eur. J.*, 2018, **34**, 8535–8541.

74 L. Plougastel, O. Koniev, S. Specklin, E. Decuypere, C. Créminon, D.-A. Buisson, A. Wagner, S. Kolodych and F. Taran, *Chem. Commun.*, 2014, **50**, 9376–9378.
75 M. Ribéraud, K. Porte, A. Chevalier, L. Madegard, A. Rachet, A. Delaunay-Moisan, F. Vinchon, P. Thuéry, G. Chiappetta, P. Alexandre Champagne, G. Pieters, D. Audisio and F. Taran, *J. Am. Chem. Soc.*, 2023, **145**, 2219–2229.
76 M. Louis, G. Force, T. D'Anfray, E. Bourgeat, E. Romero, P. Thuéry, D. Audisio, A. Sallustrau and F. Taran, *Chem. – Eur. J.*, 2024, e202302713.
77 S. Saidjalolov, E. Braud, Z. Edoo, L. Iannazzo, F. Rusconi, M. Riomet, A. Sallustrau, F. Taran, M. Arthur, M. Fonvielle and M. Etheve-Quelquejeu, *Chem. – Eur. J.*, 2021, **27**, 7687–7695.
78 I. Dovgan, A. Hentz, O. Koniev, A. Ehkirch, S. Hessmann, S. Ursuegui, S. Delacroix, M. Riomet, F. Taran, S. Cianférani, S. Kolodych and A. Wagner, *Chem. Sci.*, 2020, **11**, 1210–1215.
79 V. Lehot, O. Lidicky, J. Most, S. Erb, I. Dovgan, A. Osypenko, O. Koniev, S. Kolodych, L. Kotrchová, G. Chaubet, S. Cianférani, T. Etrych and A. Wagner, *ACS Omega*, 2023, **8**, 40508–40516.
80 E. Decuypère, M. Riomet, A. Sallustrau, S. Bregant, R. Thai, G. Pieters, G. Clavier, D. Audisio and F. Taran, *Chem. Commun.*, 2018, **54**, 10758–10761.
81 M. Riomet, K. Porte, A. Wijkhuisen, D. Audisio and F. Taran, *Chem. Commun.*, 2020, **56**, 7183–7186.
82 W. Xu, Z. Shao, C. Tang, C. Zhang, Y. Chen and Y. Liang, *Org. Biomol. Chem.*, 2022, **20**, 5953–5957.
83 F. Liu, D. I. Danylchuk, B. Andreiuk and A. S. Klymchenko, *Chem. Sci.*, 2022, **13**, 3652–3660.
84 J. Baudet, E. Lesur, M. Ribéraud, A. Chevalier, T. D'Anfray, P. Thuéry, D. Audisio and F. Taran, *Chem. Commun.*, 2024, **60**, 3657–3660.
85 (*a*) Q. Fu, S. Shen, P. Sun, Z. Gu, Y. Bai, X. Wang and Z. Liu, *Chem. Soc. Rev.*, 2023, **52**, 7737–7772; (*b*) Q. Min and X. Ji, *J. Med. Chem.*, 2023, **66**, 16546–16567.
86 Z. Shao, W. Liu, H. Tao, F. Liu, R. Zeng, P. A. Champagne, Y. Cao, K. N. Houk and Y. Liang, *Chem. Commun.*, 2018, **54**, 14089–14092.
87 W. Xu, H. Yu, R. Zhao and Y. Liang, *Bioorg. Med. Chem. Lett.*, 2023, **81**, 129129.
88 M. Feng, L. Madegard, M. Riomet, M. Louis, P. A. Champagne, G. Pieters, D. Audisio and F. Taran, *Chem. Commun.*, 2022, **58**, 8500–8503.
89 K. Porte, B. Renoux, E. Péraudeau, J. Clarhaut, B. Eddhif, P. Poinot, E. Gravel, E. Doris, A. Wijkhuisen, D. Audisio, S. Papot and F. Taran, *Angew. Chem., Int. Ed.*, 2019, **58**, 6366–6370.
90 L. Madegard, M. Girard, B. R. Yaw, K. Porte, D. Audisio, S. Papot and F. Taran, *Chem. – Eur. J.*, 2023, **29**, e202301359.
91 L. Madegard, M. Girard, E. Blochouse, B. Riss Yaw, A. Palazzolo, M. Laquembe, D. Audisio, P. Poinot, S. Papot and F. Taran, *Angew. Chem., Int. Ed.*, 2025, e202422627.
92 X. Yan, K. Li, T.-Q. Xie, X.-K. Jin, C. Zhang, Q.-R. Li, J. Feng, C.-J. Liu and X.-Z. Zhang, *Angew. Chem., Int. Ed.*, 2024, **63**, e202318539.
93 M. Ribéraud, E. Porret, A. Pruvost, F. Theodoro, A. L. Nguyen, S. Specklin, D. Kereselidze, C. Denis, B. Jego, P. Barbe, M. Keck, T. D'Anfray, B. Kuhnast, D. Audisio, C. Truillet and F. Taran, *Chem. Sci.*, 2024, **15**, 18825–18831.
94 See for example: (*a*) R. Rossin, R. M. Versteegen, J. Wu, A. Khasanov, H. J. Wessels, E. J. Steenbergen, W. ten Hoeve, H. M. Janssen, A. H. A. M. van Onzen, P. J. Hudson and M. S. Robillard, *Nat. Commun.*, 2018, **9**, 1484–1495; (*b*) R. Rossin, S. M. J. van Duijnhoven, W. ten Hoeve, H. M. Janssen, F. J. M. Hoeben, R. M. Versteegen and M. S. Robillard, *Bioconjugate Chem.*, 2016, **27**, 1697–1706; (*c*) R. M. Versteegen, R. Rossin, W. ten Hoeve, H. M. Janssen and M. S. Robillard, *Angew. Chem., Int. Ed.*, 2013, **52**, 14112–14116.
95 J. M. McFarland, M. Aleĉković, G. Coricor, S. Srinivasan, M. Tso, J. Lee, T.-H. Nguyen and J. M. Mejia Oneto, *ACS Cent. Sci.*, 2023, **9**(7), 1400–1408.